

Electronic Structure and Thermochemical Properties of Silicon-Doped Lithium Clusters $\text{Li}_n\text{Si}^{0/+}$, $n = 1-8$: New Insights on Their Stability

Truong Ba Tai^[a] and Minh Tho Nguyen^{*[a,b]}

A theoretical investigation on small silicon-doped lithium clusters Li_nSi with $n = 1-8$, in both neutral and cationic states is performed using the high accuracy CCSD(T)/complete basis set (CBS) method. Location of the global minima is carried out using a stochastic search method and the growth pattern of the clusters emerges as follows: (i) the species Li_nSi with $n \leq 6$ are formed by directly binding one Li to a Si of the smaller cluster Li_{n-1}Si , (ii) the structures tend to have an as high as possible symmetry and to maximize the coordination number of silicon. The first three-dimensional global minimum is found for Li_4Si , and (iii) for Li_7Si and Li_8Si , the global minima are formed by capping Li atoms on triangular faces of Li_6Si (O_h). A maximum coordination number of silicon is found to be 6 for the global minima, and structures with higher coordination of silicon exist but are less stable. Heats of formation at 0 K ($\Delta_f H^0$) and 298 K ($\Delta_f H^{298}$), average binding energies (E_b),

adiabatic (AIE) and vertical (VIE) ionization energies, dissociation energies (D_e), and second-order difference in total energy ($\Delta^2 E$) of the clusters in both neutral and cationic states are calculated from the CCSD(T)/CBS energies and used to evaluate the relative stability of clusters. The species Li_4Si , Li_6Si , and Li_5Si^+ are the more stable systems with large HOMO–LUMO gaps, E_b , and $\Delta^2 E$. Their enhanced stability can be rationalized using a modified phenomenological shell model, which includes the effects of additional factors such as geometrical symmetry and coordination number of the dopant. The new model is subsequently applied with consistency to other impure clusters Li_nX with $\text{X} = \text{B}, \text{Al}, \text{C}, \text{Si}, \text{Ge}$, and Sn . © 2012 Wiley Periodicals, Inc.

DOI: 10.1002/jcc.22911

Introduction

Clusters of the elements are of considerable current interest as genuine intermediates between atoms and bulk solid. A good understanding of these interesting materials gives not only more insight into the chemical and physical properties of solid but also is imperative for the design of new types of self-assembled nanomaterials. It is well known that the stability and properties of clusters strongly depend on their sizes. Enhanced stabilities are observed at a few special sizes with high abundance in mass spectroscopic experiments as compared to other neighbors. To interpret this intriguing character, some theoretical models and electron counting rules were proposed. Of the latter, the phenomenological shell model (PSM) that was originally proposed by de Heer and coworkers in 1984^[1] has been proved to be an effective model to account for the electronic structure and stability pattern of simple metal clusters.^[2–4] In the framework of PSM, the valence electrons are assumed to be freely itinerant in a simple mean-field potential that is formed by the nuclei of atoms. Accordingly, a higher stability of a metal cluster is achieved if its electronic shell or subshells are closed, and the number of valence electrons corresponds to a shell closing such as 2 ($1s^2$), 8 ($1s^2 1p^6$), 20 ($1s^2 1p^6 1d^{10} 2s^2$), and so forth, that are called the magic numbers. Recently, the simple PSM has been extensively applied for impure clusters with a modification, called the Wood–Saxon potential.^[5,6] According to this modified model, the dopant induces a perturbation and the order-

ing of the single particle energy levels is changed either to ($1s^2 1p^6 2s^2 1d^{10} 2p^6$) if the impurity is more electronegative than the host atoms, or to ($1s^2 1p^6 1d^{10} 2s^2 1f^{14} 2p^6$) if the central dopant is less electronegative. Through the PSM model, the electronic structure and stability motifs of many metal clusters were consistently rationalized, including the doped lithium clusters Li_nM with impurities M as beryllium (Be), magnesium (Mg),^[7] boron (B),^[8,9] aluminum (Al),^[10] carbon (C),^[11] tin (Sn),^[12] germanium (Ge),^[13] and oxygen (O).^[14] However, the model cannot be applied when the number of valence electrons of enhanced stability species is not the same for different systems. For the impure lithium clusters doped by group IIA and IIIA elements (Be, Mg, B, and Al),^[7–10] the most stable species are found to possess eight valence electrons, occupying orbitals of $1s^2$ and $2p^6$ in the PSM. This magic number of eight valence electrons is observed in cases of Li_nGe ^[13] and Li_nSn ,^[12] but it is failed for carbon-doped lithium clusters

[a] T. B. Tai, M. T. Nguyen
Department of Chemistry, Katholieke Universiteit Leuven, B-3001 Leuven, Belgium

[b] M. T. Nguyen
Institute for Computational Science and Technology, Thu Duc, Ho Chi Minh City, Vietnam
E-mail: minh.nguyen@chem.kuleuven.be, Fax: (+32) 16327992

Contract/grant sponsors: GOA, IDO, and IUAP programs of K.U. Leuven Research Council and ICST (to M.T.N., for his stays in Vietnam) and Arenberg Doctoral School (to T.B.T., for a scholarship)

© 2012 Wiley Periodicals, Inc.

Li_nC in which the Li_6C with 10 valence electrons is enhanced stable system.^[11] A legitimate question arises as to whether beside the number of valence electrons, there are other factors governing the cluster stability. In an attempt to obtain more insights into this question, we examine the silicon-doped lithium clusters Li_nSi under a PSM viewpoint, followed by an extended comparison to similar systems.

As the theoretical prediction for the existence of CLi_6 ^[15] was experimentally confirmed,^[16] the group IVA element-doped lithium clusters have extensively been studied by many groups. Although doped lithium clusters Li_nX with impurities X including carbon (C),^[11,15–19] germanium (Ge),^[13] and tin (Sn)^[12,20] were carefully studied, investigations on silicon derivatives are more limited. According to our best knowledge, results on some special sizes Li_nSi with $n = 4$ and 6 were previously reported.^[21–23] Recently, He et al.^[24] reported an investigation of structure and stability on lithium monosilicide clusters Li_nSi ($n = 4–16$). Similar to the Li_nC isovalent systems, these authors found that the Li_6Si is the most stable species and the special stability of Li_6Si was explained in terms of a “magic number of coordination.” However, the small clusters Li_nSi with $n \leq 3$ that are important to understand the chemical bonding were not reported. Moreover, the charged clusters Li_nSi^+ , being interesting targets for experimental spectrometric studies, have not been considered in previous reports.

Overall, a uniform and consistent view of the structure and stability of the small Li_nSi clusters is still missing. In this context, we set out to perform systematically a theoretical investigation of a series of small silicon-doped lithium clusters Li_nSi with n ranging from 1 to 8, at both neutral and cationic states using quantum chemical computations at the B3LYP and CCSD(T) levels. Energetic properties are determined using coupled-cluster theory CCSD(T) in conjunction with the correlation-consistent aug-cc-pVnZ basis sets, and extrapolated to the complete basis set (CBS) limit. In view of the lack of experimental values for Li_nSi clusters, the standard heats of formation are evaluated. Stability of the doped lithium clusters Li_nSi is evaluated in comparison to that of the corresponding pure lithium clusters. The stability motif of clusters is subsequently rationalized on the basis of the PSM, which is adjusted by considering the coordination number of the dopant and structural symmetry. The resulting proposition is subsequently applied to other impure lithium clusters Li_nX with X = Be, Mg, B, Al, C, Ge, and Sn, and this gives additional insights into the factors governing the stability of mixed lithium clusters.

Computational Methods

All standard electronic structure calculations are carried out using the Gaussian 03^[25] and Molpro 2008^[26] program packages. For small clusters $\text{Li}_n\text{Si}^{0/+}$, $n = 1–4$, with a limited number of isomers, the initial structures are generated manually. The initial search for all possible low-lying isomers of the larger systems $\text{Li}_n\text{Si}^{0/+}$ with $n = 5–8$ is performed using a stochastic search algorithm that was implemented by us.^[27] First, possible structures of each $\text{Li}_n\text{Si}^{0/+}$ are generated by the random “kick” method and then rapidly optimized using the density functional theory with the

hybrid B3LYP functional^[28–30] in conjunction with the small 6-31G basis set.^[31] In this kick procedure, the minimum and maximum distances between atoms are limited to 2 and 8 Å, respectively. With about 100 structures for each of clusters $\text{Li}_n\text{Si}^{0/+}$ generated by kick procedure, the number of minima effectively located after optimization is around 80 in which the lower lying isomers are repeated many times. Equilibrium geometries and harmonic vibrational frequencies of the lower lying isomers in both neutral and cationic states are further calculated at the B3LYP/6-311+G(d) level.^[32] To improve the calculated results, geometries of the lowest energy isomers of all clusters and their vibrational frequencies are refined at the coupled-cluster theory CCSD(T) level^[32–35] with the correlation-consistent aug-cc-pVTZ basis set and the R/UCCSD(T) approach for opened shell species. The valence electronic energies are computed using CCSD(T) with the aug-cc-pVnZ basis sets, which are denoted as aVnZ with $n = \text{D, T, and Q}$. The aVnZ basis set is the combination of the cc-pVnZ basis set for Li^[36] and aug-cc-pVnZ basis set for Si.^[37] The CCSD(T) energies are subsequently extrapolated to the CBS limit by using fitting eq. (1).^[38]

$$E(x) = A_{\text{CBS}} + B \exp [-(x-1)] + C \exp [-(x-1)^2], \quad (1)$$

where $x = 2, 3$, and 4 for the aVnZ basis sets, D, T, and Q, respectively.

The core-valence correlation corrections to the CCSD(T) energies for the core electrons on Li and Si are calculated at the CCSD(T)/cc-pwCVTZ level.^[39] Douglas–Kroll–Hess (DKH) scalar relativistic corrections ($\Delta E_{\text{DKH-SR}}$), which account for changes in the relativistic contributions to the total energies of the molecule and the constituent atoms, are calculated using the spin-free one-electron DKH Hamiltonian.^[40,41] $\Delta E_{\text{DKH-SR}}$ is defined as the difference in the total energy between the results obtained from basis sets recontracted for DKH calculations^[41] and the total energy obtained with the normal valence basis set of the same quality. The DKH calculations are obtained as the differences of the results from the CCSD(T)/aug-cc-pVTZ and the CCSD(T)/aug-cc-pVTZ-DK levels.^[42] Finally, a spin-orbit (SO) correction of 0.43 kcal/mol for the Si atom obtained from the excitation energies of Moore^[43] is used. SO correction of Li atom is equal to zero due to its outer valence configuration $2s^1$. The total atomization energy (ΣD_0 or TAE) of a compound is given by eq. (2):

$$\Sigma D_0 = \Delta E_{\text{CBS}} + \Delta E_{\text{CV}} + \Delta E_{\text{DKH-SR}} + \Delta E_{\text{SO}} - \Delta E_{\text{ZPE}} \quad (2)$$

By combining our computed ΣD_0 values with the known heats of formation at 0 K for the elements Si and Li, we can derive $\Delta_f H_0$ values at 0 K for the corresponding molecules in the gas phase. In this work, we use the values at 0 K of $\Delta_f H(\text{Si}) = 107.2 \pm 0.2$ kcal/mol^[44] and $\Delta_f H(\text{Li}) = 37.7 \pm 0.2$ kcal/mol.^[45] Heats of formation at 298 K are calculated by following a classical thermochemical procedure.^[46]

Results and Discussion

In view of the severe lack of available experimental results for Li_nSi , the diatomic Li_2 and Si_2 are first studied as a preliminary calibration, using the same methods and their calculated results

are compared with previous theoretical and experimental results. Heats of formation at 0 and 298 K of diatomic Li_2 , Si_2 , and the $\text{Li}_n\text{Si}^{0/+}$ clusters, derived from TAEs together with the corrections, are given in Table 1. The CCSD(T) total energies using the aVnZ ($n = \text{D, T, and Q}$) basis sets and the limit CBS

clusters Li_nSi^+ are shown in Figure 2. As for a convention, the lower lying structures are labeled hereafter by **nn.X** and **nc.X** where the first letter **n** stands for the cluster size (Li_nSi), the second letter **n** for a neutral species, **c** for a cationic one, and **X** for the number of isomer presented.

Table 1. Heats of formation at 0 K ($\Delta_f H^0$) and 298 K ($\Delta_f H^{298}$), TAEs and different components (kcal/mol) for neutral Li_nSi and cationic Li_nSi^+ clusters ($n = 1\text{--}8$) using CCSD(T)/CBS energies.

Structures	CBS ^[a]	ZPE ^[b]	$\Delta\text{SR}^{[c]}$	$\Delta\text{core}^{[d]}$	$\Delta\text{SO}^{[e]}$	TAE	$\Delta_f H^0$	$\Delta_f H^{298}$
Li_2 ($^1\Sigma_g^+$)	24.2	0.5	0.0	0.2	0.0	23.8 (24.1) ^[f]	51.6 (51.6 \pm 0.7) ^[g]	51.7
Si_2 ($^3\Sigma_g^-$)	75.5	0.7	−0.2	0.3	−0.86	74.0	140.4 (139 \pm 1.7) ^[h]	141.1
LiSi^+ ($\text{C}_{\infty\text{v}}$, $^3\Pi$)	−106.5	0.4	0.0	−0.5	−0.43	−107.8	252.7	253.2
LiSi ($\text{C}_{\infty\text{v}}$, $^4\Sigma_g^-$)	43.3	0.6	−0.2	0.1	−0.43	42.1	102.8	103.1
Li_2Si^+ ($\text{D}_{\infty\text{h}}$, $^2\Pi$)	−38.5	1.4	−0.2	−0.3	−0.43	−40.9	223.5	224.0
Li_2Si ($\text{D}_{\infty\text{h}}$, $^3\Sigma_g^+$)	81.0	1.5	−0.3	0.4	−0.43	79.1	103.5	103.9
Li_3Si^+ ($\text{D}_{3\text{h}}$, $^1\text{A}_1'$)	13.8	2.3	−0.3	0.0	−0.43	10.7	209.6	209.8
Li_3Si ($\text{C}_{2\text{v}}$, $^2\text{B}_1$)	120.4	2.3	−0.3	1.0	−0.43	118.3	102.0	101.6
Li_4Si^+ ($\text{D}_{4\text{h}}$, $^2\text{A}_{2\text{u}}$)	67.8	3.3	−0.4	0.7	−0.43	64.3	193.7	193.3
Li_4Si ($\text{C}_{2\text{v}}$, $^1\text{A}_1$)	169.2	3.6	−0.3	1.7	−0.43	166.5	91.5	91.4
Li_5Si^+ ($\text{D}_{3\text{h}}$, $^1\text{A}_1'$)	120.0	4.1	−0.5	1.3	−0.43	116.2	179.5	178.5
Li_5Si ($\text{C}_{4\text{v}}$, $^2\text{A}_1$)	203.8	4.4	−0.3	2.2	−0.43	200.9	94.8	94.7
Li_6Si^+ (O_h , $^2\text{A}_{1\text{g}}$)	150.2	4.8	−0.4	1.8	−0.43	146.4	187.0	187.3
Li_6Si (O_h , $^1\text{A}_{1\text{g}}$)	239.7	4.5	−0.3	2.5	−0.43	236.9	96.5	97.0
Li_7Si^+ ($\text{C}_{3\text{v}}$, $^1\text{A}_1$)	172.9	5.5	−0.3	2.2	−0.43	168.9	202.2	202.5
Li_7Si^+ ($\text{C}_{3\text{v}}$, $^1\text{A}_1$)	181.3	6.2	−0.5	2.4	−0.43	176.6	194.5	193.8
Li_7Si (C_s , $^2\text{A}'$)	262.7	6.0	−0.4	3.1	−0.43	259.0	112.1	112.1
Li_7Si ($\text{C}_{2\text{v}}$, $^2\text{A}_1$)	257.6	5.6	−0.3	3.1	−0.43	254.3	116.8	117.0
Li_8Si^+ (C_1 , ^2A)	202.0	6.9	−0.4	3.0	−0.43	197.3	211.5	211.5
Li_8Si^+ ($\text{D}_{3\text{d}}$, $^2\text{A}_{2\text{u}}$)	171.8	6.4	−0.4	2.4	−0.43	167.0	241.8	242.1
Li_8Si ($\text{C}_{2\text{v}}$, ^1A)	295.1	7.1	−0.4	3.6	−0.43	290.8	118.0	117.8
Li_8Si ($\text{C}_{2\text{v}}$, $^1\text{A}_1$)	289.6	6.5	−0.3	3.4	−0.43	285.7	123.1	123.3
Li_8Si (C_s , $^1\text{A}'$)	290.1	6.5	−0.3	3.5	−0.43	286.3	122.5	122.7

[a] Extrapolated by using eq. (1) with the aVnZ basis sets ($n = \text{D, T, and Q}$). [b] Zero point energies taken from the CCSD(T)/aVTZ harmonic frequencies for clusters $\text{Li}_n\text{Si}^{0/+}$ ($n = 1\text{--}8$). [c] Scalar relativistic correction based on a CCSD(T)-DK/aug-cc-pVTZ-DK calculation expressed relative to the CCSD(T) result without the DK correction. [d] Core-valence corrections obtained with the cc-pwCVTZ basis sets at the optimized CCSD(T) geometries. [e] Correction due to the incorrect treatment of the atomic asymptotes as an average of spin multiplets. Values based on C. Moore's Tables, Ref. [43]. [f] The experimental values obtained from Ref. [47]. [g] The experimental values obtained from Ref. [49]. [h] The experimental values obtained from Ref. [50].

values obtained are shown in Table S1 of the Supporting Information file. It can be observed that there is a small difference between our calculated values and available experimental values (Table 1). The dissociation energy of the Li_2 ($^1\Sigma_g^+$) of 23.8 kcal/mol agrees well with the experimental value of 24.1 kcal/mol.^[47] Previous theoretical values include those of 22.1 kcal/mol (MP4/6-311+G(2df)) and 23.6 kcal/mol (QCISD(T)/6-311+G(2df)).^[48] The heat of formation at 0 K of the diatomic Li_2 ($^1\Sigma_g^+$) calculated from TAE is 51.6 kcal/mol that coincides with the experimental value of 51.6 \pm 0.7 kcal/mol.^[49] Similarly, the heat of formation at 0 K of the Si_2 ($^3\Sigma_g^-$) of 140.4 kcal/mol is in good agreement with the experimental value of 139.6 \pm 1.7 kcal/mol (584 \pm 7 kJ/mol).^[50] Because of the lack of available experimental data, this agreement for the diatomic Li_2 and Si_2 lends us a confidence in the thermal functions calculated for other clusters, and allows an estimate on the accuracy of the calculated results, that is expected to be \pm 2.0 kcal/mol.

Shapes of the low-lying isomers Li_nSi and growth mechanism

While the shape, point group, number of imaginary frequencies, and relative energy (kcal/mol) of each of the lower lying Li_nSi isomers are depicted in Figure 1, those of the cationic

The high spin **1n.1** ($^4\Sigma^-$) with the electron configuration of [$1\sigma^2 2\sigma^1 1\pi^2$] is found to be the ground state for the diatomic LiSi with doublet–quartet gap of 8.1 kcal/mol. This observation is consistent with the fact that Li tends to donate one electron to Si and form the ionic bond between two of these atoms. Consequently, the electron configuration of LiSi is similar to that of the Si^- anion in which valence electrons of p-subshell are distributed in three 2p-orbitals.

Similar to the cases of $\text{Li}_2\text{C}^{[11]}$ and $\text{Li}_2\text{Ge}^{[13]}$ a linear form LiSiLi with high spin state **2n.1** ($^3\Sigma_g^+$) is found to be the lowest energy isomer for Li_2Si . The next isomer is a bent triplet **2n.2** ($\text{C}_{2\text{v}}$, $^3\text{A}_2$) with a relative energy of 5.2 kcal/mol.

For Li_3Si , the planar structure **3n.1** ($\text{C}_{2\text{v}}$, $^2\text{B}_1$) that is formed by directly binding one Li to Si of the linear form LiSiLi **2n.1** is the most stable isomer. While the symmetrical doublet **3n.2** ($\text{D}_{3\text{h}}$, $^2\text{A}_1''$) turns out to be a second-order saddle point with two imaginary frequencies, the three-dimensional structure **3n.3** ($\text{C}_{3\text{v}}$, $^4\text{A}_1$) is the next isomer with a relative energy of 19.8 kcal/mol.

In agreement with previous reports,^[21,23,24] the structures **4n.1** ($\text{C}_{2\text{v}}$, $^1\text{A}_1$), **5n.1** ($\text{C}_{4\text{v}}$, $^2\text{A}_1$), and **6n.1** (O_h , $^1\text{A}_{1\text{g}}$) are found to be the global minima for the neutrals Li_4Si , Li_5Si , and Li_6Si , respectively. For these sizes, other structures given in Figure 1

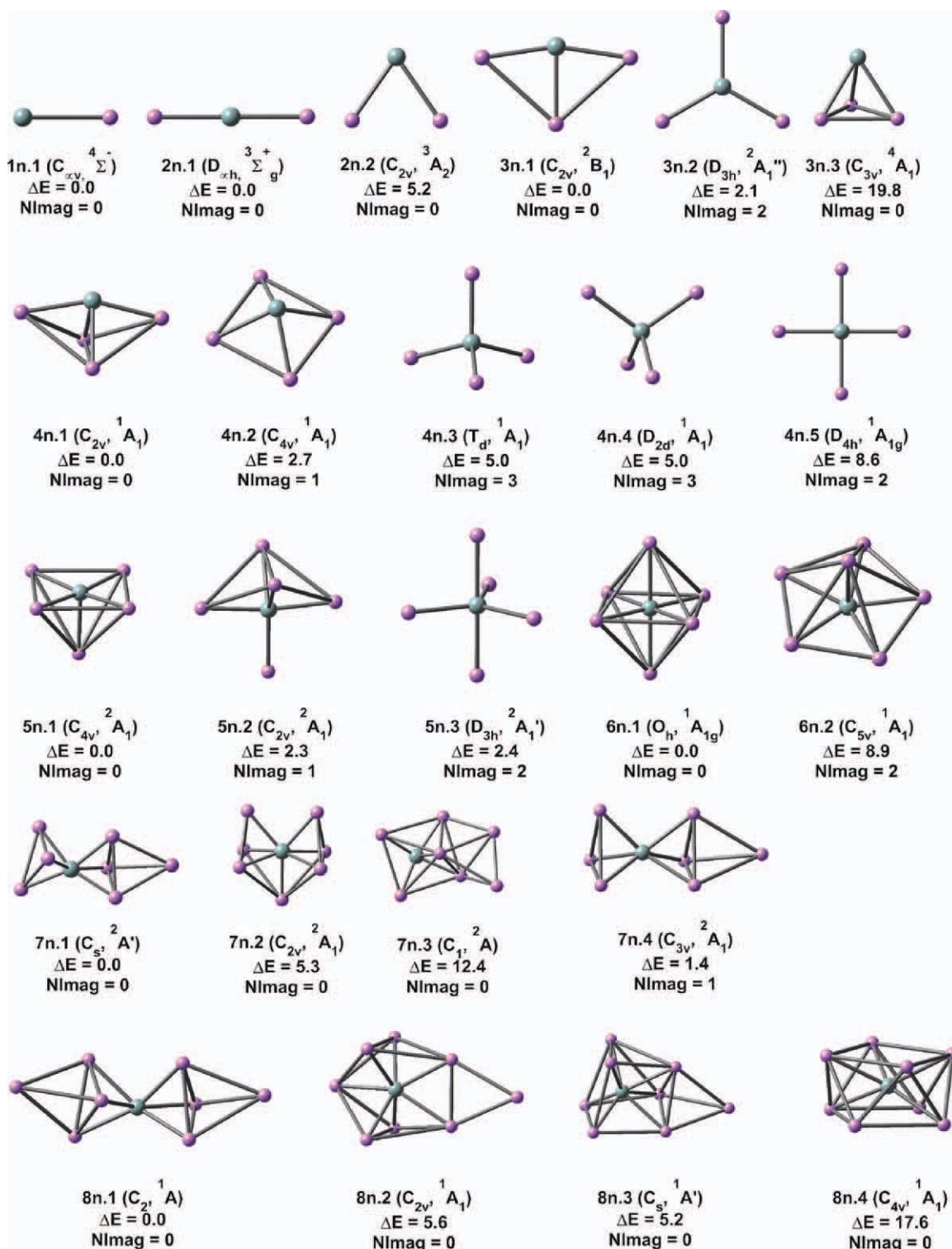


Figure 1. Optimized structures of the clusters Li_nSi ($n = 1-8$) and relative energies at 0 K (ΔE , kcal/mol including ZPEs) calculated at the B3LYP/6-311+G(d) level. [Color figure can be viewed in the online issue, which is available at wileyonlinelibrary.com.]

are either a transition state or a second-order saddle point with one or two imaginary frequencies. A global minimum Li_nSi ($n = 4-6$) can in general be formed by binding directly one Li to Si of the $Li_{n-1}Si$ minimum.

Three different isomers, namely from **7n.1** to **7n.3**, are located for Li_7Si . It is interesting to note that the structure

7n.1 ($C_{5v}, {}^2A'$) in which one Li atom is capped on one of the triangular faces of Li_6Si (**6n.1**) is the lowest lying isomer for Li_7Si . Its C_{3v} counterpart **7n.4** ($C_{3v}, {}^2A_1$) turns out to be a transition state with one imaginary frequency. The structure **7n.2** ($C_{2v}, {}^2A_1$) in which Si is directly bound to all Li atoms and has a coordination number of 7 is the next isomer with a relative

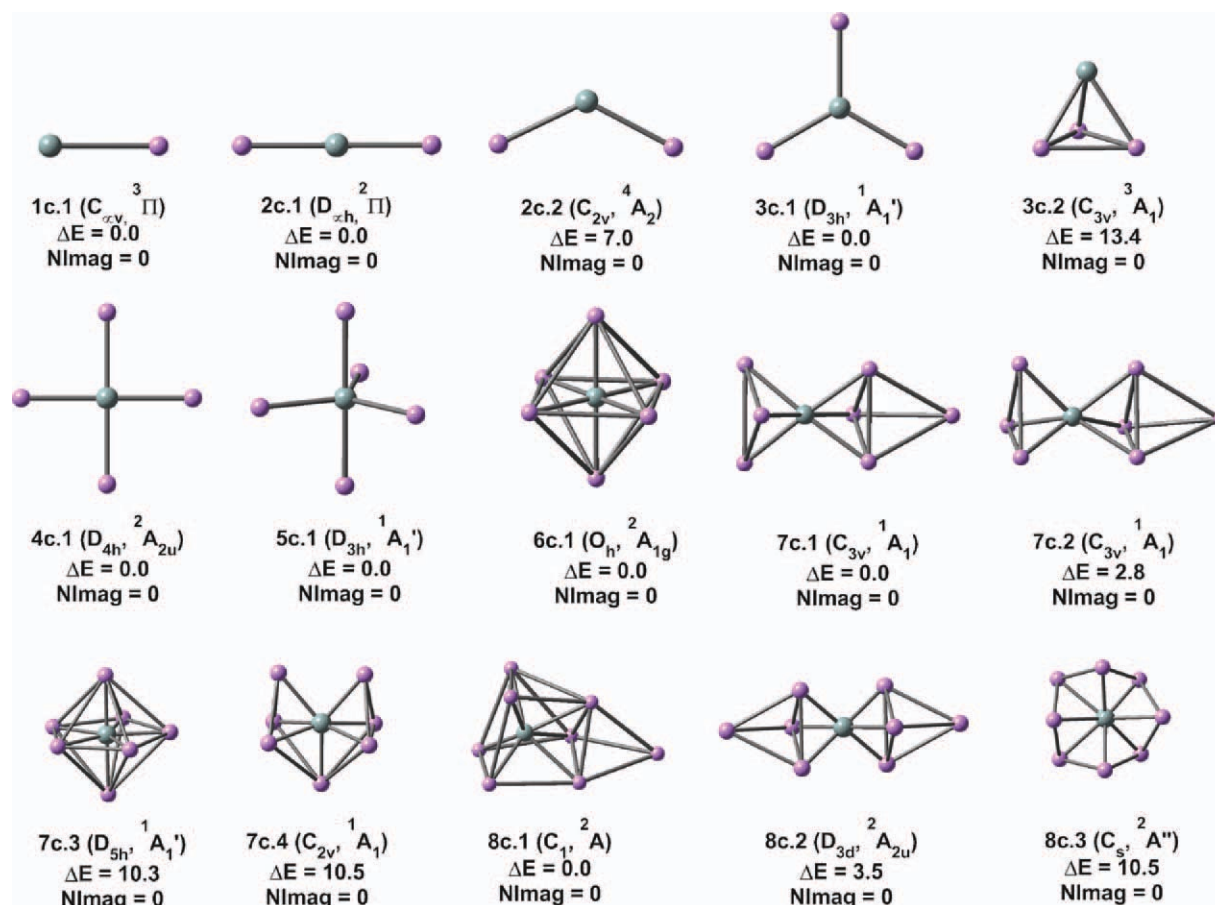


Figure 2. Optimized structures of the cationic clusters Li_nSi^+ ($n = 1-8$) and relative energies at 0 K (ΔE , kcal/mol including ZPEs) calculated at the B3LYP/6-311+G(d) level. [Color figure can be viewed in the online issue, which is available at wileyonlinelibrary.com.]

energy of 5.3 kcal/mol. The structure **7n.3** in which Si is located outside the Li_n framework is 12.4 kcal/mol less stable than **7n.1**.

The global minimum of Li_8Si is a C_2 structure **8n.1** in which two Li atoms are capped on two opposite triangular faces of Li_6Si (O_h). Similar to the case of Li_7Si , the coordination number of silicon is only equal to 6 in **8n.1**. Two structures **8n.2** ($C_{2v}, {}^1A_1$) and **8n.3** ($C_s, {}^1A'$) that are formed by adding one excess Li into Li_7Si (**7n.2**) are the next low-lying isomers with a coordination number of 7, whereas the high symmetry **8n.4** ($C_{4v}, {}^1A_1$) in which Si is located at the center of the antiprism square cage Li_8 is much less stable with relative energy of 17.8 kcal/mol.

Generally, the growth pattern for small Li_nSi clusters with $n = 1-8$ can be formulated as follows: (i) a small cluster Li_nSi with $n \leq 6$ is formed by directly binding one excess Li to Si of the smaller $Li_{n-1}Si$, (ii) the structures tend to have an as high as possible symmetry and to maximize the coordination number of silicon. The first three-dimensional global minimum is found for Li_4Si , and (iii) for the larger clusters Li_7Si and Li_8Si , both global minima are formed by capping Li on triangular faces of Li_6Si (O_h). The maximal number of coordination of silicon is found to be 6 for the global minima, and the structures with a higher coordination number of silicon are less favorable.

Shapes of the low-lying cationic isomers Li_nSi^+

Following detachment of one electron, the structures of small cationic clusters are slightly distorted from those of their corresponding neutrals (Fig. 2). The triplet ${}^3\Pi$ with a valence electron configuration of $[1\sigma^1 1\pi^1]$ is the ground state for cation $LiSi^+$. The low spin ${}^1\Sigma^+$ is 7.2 kcal/mol higher in energy.

Similarly, the low spin state of linear triatomic $LiSiLi$ **2c.1** (${}^2\Pi$) is the most stable isomer for cation Li_2Si^+ . The next isomer is a high spin **2c.2** (4A_2), whereas its doublet (2B_2) is much less stable with a relative energy of 16.3 kcal/mol.

Detachment of one electron from SOMO of the high symmetry tetra-atomic structure **3n.2** (D_{3h}) leads to a disappearance of the Jahn-Teller effect. Consequently, the high symmetry low spin **3c.1** ($D_{3h}, {}^1A_1'$) is indicated to be the most stable isomer, whereas the high spin **3c.2** ($C_{3v}, {}^3A_1$) is the next isomer at 13.4 kcal/mol.

For larger clusters Li_nSi^+ with $n = 4-6$, we found that a squared planar structure **4c.1** ($D_{4h}, {}^2A_{2u}$) in which Si is located at the center of the square Li_4 is the most stable isomer for Li_4Si^+ . Two structures **5c.1** ($D_{3h}, {}^1A_1'$) and **6c.1** ($O_h, {}^2A_{1g}$) are the global minima of Li_5Si^+ and Li_6Si^+ , respectively.

Our calculations show that a C_{3v} structure **7c.1**, which is a higher symmetry form of the neutral **7n.1** (C_s), is the global minimum for Li_7Si^+ . The C_{3v} structure **7c.2** is the next isomer

Table 2. HOMO-LUMO gap (HLG, eV), average binding energy (E_b , eV), and dissociation energies (D_e , eV) of various reactions for the neutrals Li_nSi and cations Li_nSi^+ using CCSD(T)/CBS energies.

Neutrals	HLG	E_b	$D_e(7)$	$D_e(8)$	Cations	HLG	E_b	$D_e(9)$	$D_e(10)$	$D_e(11)$	$D_e(12)$
LiSi ($C_{\infty v}$, $4\sum^-$)	–	0.91	1.88	1.88	LiSi^+ ($C_{\infty v}$, 3Π)	–	0.36	3.52	0.72	3.52	0.72
Li_2Si ($D_{\infty h}$, $3\sum_g^+$)	–	1.14	2.46	1.63	Li_2Si^+ ($D_{\infty h}$, 2Π)	–	1.21	2.95	1.79	5.42	2.39
Li_3Si (C_{2v} , $2B_1$)	–	1.28	3.58	1.71	Li_3Si^+ (D_{3h} , $1A_1'$)	1.898	1.47	2.27	2.43	7.10	3.03
Li_4Si (C_{2v} , $1A_1$)	1.860	1.44	4.38	2.12	Li_4Si^+ (D_{4h} , $2A_{2u}$)	–	1.64	2.34	3.06	8.12	4.64
Li_5Si (C_{4v} , $2A_1$)	–	1.45	4.97	1.50	Li_5Si^+ (D_{3h} , $1A_1'$)	2.622	1.74	2.26	3.21	9.47	5.36
Li_6Si (O_h , $1A_{1g}$)	1.540	1.47	5.13	1.55	Li_6Si^+ (O_h , $2A_{1g}$)	–	1.68	1.31	3.02	9.39	5.54
Li_7Si (C_{3v} , $2A'$)	–	1.40	4.82	1.00	Li_7Si^+ (C_{3v} , $1A_1$)	2.015	1.65	1.49	2.95	9.57	5.39
Li_8Si (C_{2v} , $1A$)	1.765	1.38	4.98	1.41	Li_8Si^+ (C_{1v} , $2A$)	–	1.55	0.76	2.71	9.08	5.19

with a small relative energy of 2.8 kcal/mol. Two isomers, namely **7c.3** (D_{5h} , $1A_1'$) and **7c.4** (C_{2v} , $1A_1$), are also found to be stable with 10.3 and 10.5 kcal/mol higher in energy, respectively.

For the Li_8Si^+ , the structure **8c.1** (C_1 , $2A$) which is the cationic state of the corresponding neutral **8n.3** (C_s) is found to be the most stable isomer. The **8c.2** (D_{3d} , $2A_{2u}$) located at 3.5 kcal/mol is the next isomer, whereas the **8c.3** (C_{3v} , $2A'$) that is formed by detaching one electron from the neutral **8n.4** (C_{4v}) is less stable, being at 10.5 kcal/mol.

Energetic Properties. One of the fundamental characters of metal clusters is the dependence of their relative stabilities on the size, which can be depicted by using energetic properties. In this context, the relative stabilities of Li_nSi in both neutral and cationic states are examined on the basis of the average binding energy (E_b) and the second-order difference in total energies (Δ^2E), which are defined as follows:

$$E_b(\text{Li}_n\text{Si}) = [nE(\text{Li}) + E(\text{Si}) - E(\text{Li}_n\text{Si})]/(n+1) \quad (3)$$

$$E_b(\text{Li}_n\text{Si}^+) = [(n-1)E(\text{Li}) + E(\text{Li}^+) + E(\text{Si}) - E(\text{Li}_n\text{Si}^+)]/(n+1) \quad (4)$$

$$\Delta^2E(\text{Li}_n\text{Si}) = E(\text{Li}_{n-1}\text{Si}) + E(\text{Li}_{n+1}\text{Si}) - 2E(\text{Li}_n\text{Si}) \quad (5)$$

$$\Delta^2E(\text{Li}_n\text{Si}^+) = E(\text{Li}_{n-1}\text{Si}^+) + E(\text{Li}_{n+1}\text{Si}^+) - 2E(\text{Li}_n\text{Si}^+) \quad (6)$$

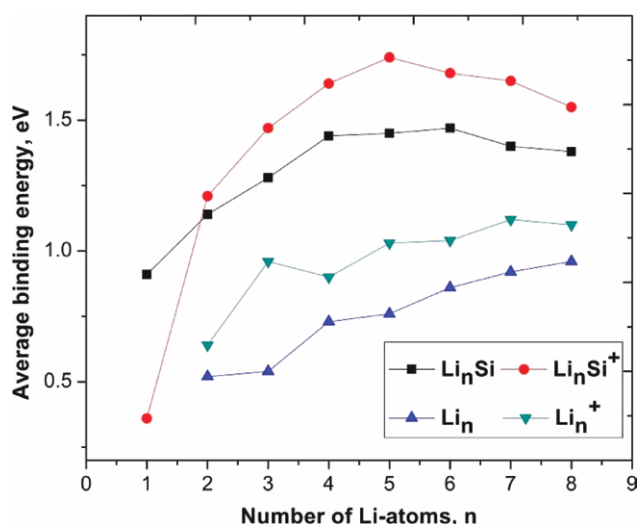


Figure 3. Average binding energy at 0 K (eV) of Li_n and Li_nSi ($n = 1-8$) in both neutral and cationic states calculated using the CCSD(T)/CBS approach.

where $E(\text{Li})$ and $E(\text{Si})$ are total energies of atoms of Li and Si, respectively. $E(\text{Li}_n\text{Si})$ and $E(\text{Li}_n\text{Si}^+)$ are total energies of neutral Li_nSi and cationic Li_nSi^+ , respectively.

To emphasize the effects of adding a silicon dopant, the average binding energy (E_b), evaluated from eqs. (3) and (4) are compared with those of pure lithium clusters Li_n . While the $E_b(\text{Li}_n\text{Si})$ values are listed in Table 2, their plots are depicted in Figure 3. The E_b values of pure lithium clusters are taken from Ref. [9] obtained using the same computational methods. At the first glance, it can be observed that the addition of silicon dopant considerably increases the E_b values of impure Li_nSi cluster as compared to those of corresponding pure hosts. This increase can be understood partly due to the larger strength of the Si–Li bond as compared to the Li–Li bond. The CBS value of 24.2 kcal/mol for the dissociation energy of diatomic Li_2 is much smaller than that of 43.3 kcal/mol of LiSi .

The E_b value tends to increase with the increasing sizes, and the maximal peaks are found at $n = 6$ for the neutrals and $n = 5$ for the cations. At the neutral state, the maximum E_b value is found for Li_6Si in which silicon directly binds to six Li atoms giving rise to an octahedral Li_6Si . The closed shell Li_4Si also reveals considerably high E_b value that is only somewhat lower than that of Li_6Si . For larger neutrals with $n = 7$, the maximum coordination number of silicon remains to be

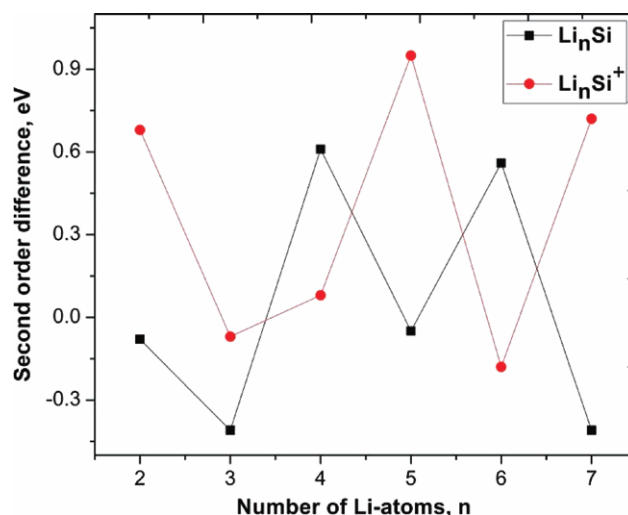


Figure 4. Second-order difference in total energy at 0 K (eV) of the Li_nSi clusters in both neutral and cationic states calculated using the CCSD(T)/CBS approach.

six, and as a consequence Si is not connected directly with all Li atoms. A consequence is that their binding energies consistently decrease. For cationic clusters, although the coordination number of silicon in the structures Li_6Si^+ and Li_8Si^+ is found to be higher than that of Li_5Si^+ , these species have opened electron shells and thereby are less stable.

The second-order difference in total energies (Δ^2E) is usually considered as a measure of the relative stability of a Li_nSi species with respect to that of its two immediate neighbors Li_{n+1}Si and Li_{n-1}Si . A larger value of Δ^2E indicates that such cluster has a higher relative stability. The curves of second-order difference in energy shown in Figure 4 reveals a consistent odd–even oscillation in which the closed shell systems show, as expected, higher stability. In consistence with findings based on the E_b values above, the maximum peaks appear at Li_4Si , Li_6Si , and Li_5Si^+ that emphasize a higher thermodynamic stability of these species. The unexpected low Δ^2E value of Li_3Si^+ can be due to a high thermodynamic stability of the product Li_2Si^+ . As shown in Table 2, the dissociation energy of the channel $\text{Li}_n\text{Si}^+ \rightarrow \text{Li}_{n-1}\text{Si}^+ + \text{Li}$ of Li_2Si^+ amount to 2.95 eV, which is larger than that of 2.27 eV of the Li_3Si^+ .

Adiabatic (AIE) and vertical (VIE) ionization energies. Adiabatic (vertical) ionization energies are confident experimental information on the geometric and electronic structure of metal clusters beside other spectrometric measures such as those from vibrational spectroscopy. The values of AIE and VIE of the clusters Li_nSi are calculated using the CBS energies together with corrections of zero point energy (ZPE), DKH scalar relativistic corrections ($\Delta E_{\text{DKH-SR}}$), and core-valence correlation (ΔE_{CV}), and are given in Table 3. There is a negligible difference

Table 3. Adiabatic (AIE) and vertical (VIE) ionization energies (eV) of Li_nSi using CCSD(T)/CBS energies.

Neutrals	Cations	AIE	Cations	VIE
LiSi ($C_{\infty v}$, $4\sum^-$)	LiSi^+ ($C_{\infty v}$, 3Π)	6.48	LiSi^+ ($C_{\infty v}$, 3Π)	6.68
Li_2Si ($D_{\infty h}$, $3\sum^+$)	Li_2Si^+ ($D_{\infty h}$, 2Π)	5.16	Li_2Si^+ ($D_{\infty h}$, 2Π)	5.26
Li_3Si (C_{2v} , $2B_1$)	Li_3Si^+ (D_{3h} , $1A_1'$)	4.57	Li_3Si^+ (C_{2v} , $1A_1$)	4.96
Li_4Si (C_{2v} , $1A_1$)	Li_4Si^+ (D_{4h} , $2A_{2u}$)	4.35	Li_4Si^+ (C_{2v} , $2B_1$)	4.90
Li_5Si (C_{4v} , $2A_1$)	Li_5Si^+ (D_{3h} , $1A_1'$)	3.59	Li_5Si^+ (C_{4v} , $1A_1$)	3.70
Li_6Si (O_h , $1A_{1g}$)	Li_6Si^+ (O_h , $2A_{1g}$)	3.85	Li_6Si^+ (O_h , $2A_{1g}$)	3.86
Li_7Si (C_{3v} , $2A_1'$)	Li_7Si^+ (C_{3v} , $1A_1$)	3.36	Li_7Si^+ (C_{3v} , $1A_1'$)	3.62
Li_8Si (C_{2v} , $1A$)	Li_8Si^+ (D_{3d} , $2A_{2u}$)	5.30	Li_8Si^+ (C_{2v} , $2A$)	4.39

between the AIE and VIE values for species LiSi , Li_2Si , and Li_6Si in which the geometries of the global minima in both neutral and cationic states are similar. This difference becomes significant for the larger sizes where geometrical distortions occur. An energetic difference of 0.55 eV for both quantities is found for Li_4Si whose geometry changes from three-dimensional Li_4Si (C_{2v}) to two-dimensional Li_4Si^+ (D_{4h}). The largest difference of 0.91 eV is associated with Li_8Si (**8n.1**, C_2) due to the lesser stability of the corresponding cation Li_8Si^+ (**8c.2**, D_{3d}).

HOMO–LUMO Gaps. The energy gaps of frontier orbitals can be considered as one of criterions to examine the stability of clusters. A large HOMO–LUMO gap (HLG) indicates that the system is unfavorable to loose electrons or to accept additional

electrons. The HLG of closed shell systems are obtained at the B3LYP/6-311+G(d) level and given in Table 2. As expected, the “magic” cluster Li_5Si^+ exhibits the highest HLG value as compared to other cationic clusters. At the neutral state, the highest HLG is found for Li_4Si (HLG = 1.9 eV) that is consistent with the enhanced stability of this eight-electron system. The energy gap of Li_6Si is slightly lower and is comparable to that of 1.6 eV of the higher congener Li_6Ge .^[13] This value is much larger than 0.8 eV of Li_6Sn that was found as an unstable cluster in the series of the tin-doped lithium clusters Li_nSn .^[12]

Dissociation Energies. To probe further the thermodynamic stability of the clusters, their various dissociation energies (D_e) are examined. For neutral ones, the dissociation energy is defined by reactions (7) and (8):



For the cations Li_nSi^+ , four dissociation channels are examined from the following reactions:



Dissociation energies (D_e) are calculated from the CBS energies with only corrections for ZPEs, and are given in Table 2. To calculate the dissociation energies of reactions (8), (11), and (12), total energies of pure lithium clusters Li_n and Li_n^+ obtained at the same CBS method are taken from Ref. [9]. The D_e values in Table 2 reveal that the dissociation energies obtained from reaction (8) are considerably lower than those from reaction (7). Accordingly, decomposition of a Li_nSi cluster tends to form one fragment Li_{n-1}Si plus one Li atom rather than one Si atom plus fragment Li_n . These observations can be understood by the fact that the Si–Li bond is stronger than that between two Li atoms. Additionally, except for $n = 2$, an odd–even trend is observed for the D_e values of reaction (8) in which closed shell systems consistently show higher D_e values as compared to those of opened shell systems.

Decomposition of the cationic clusters Li_nSi^+ to give a cationic fragments, either $\text{Li}_{n-1}\text{Si}^+$ or Li_n^+ , plus one neutral atom (Li or Si) is less endothermic. These results can easily be understood because the larger clusters can stabilize the charge better. Dissociation energies of LiSi^+ and Li_2Si^+ obtained from reaction (10) are remarkably smaller than those from reaction (9). This exception can be explained as Li tends to donate its valence electron to form the cation Li^+ . Similar to observations for neutrals, attachment of Si to form the clusters Li_nSi^+ is more exothermic than attachment of Li.

Rationalization of the enhanced stabilities

According to the above theoretical predictions, the species Li_4Si , Li_6Si , and Li_5Si^+ emerge as the systems with enhanced

stability within the series of small clusters Li_nSi ($n = 1-8$), which are characterized by large HLG, high E_b , and maximum Δ^2E peaks. The plots of total and partial density of states (DOS) for the Li_6Si given in Figure 5 reveal that 10 valence

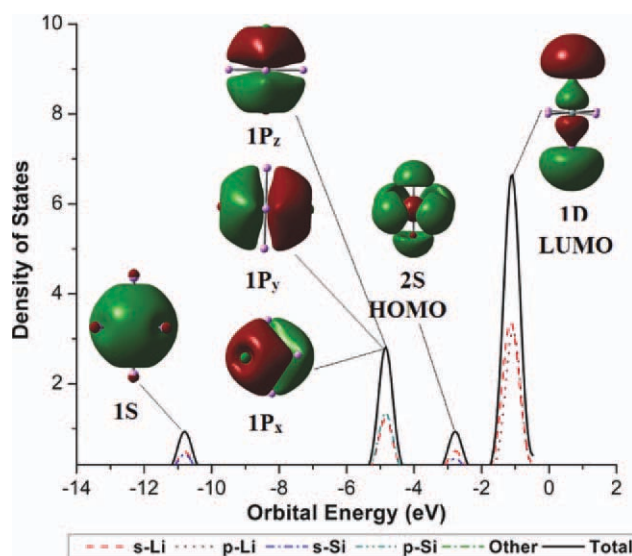


Figure 5. The plot of density of states of Li_6Si (**6n.1**) using MOs obtained at the B3LYP/6-311+G(d) level.

electrons of Li_6Si (O_h) are arranged following an electron shell ordering of $[1S^2 1P^6 2S^2 1D^0]$. The lowest orbital of Li_6Si is an s-type orbital that is composed of the s-AOs of both lithium and silicon atoms. They are followed by three degenerate p-type orbitals that mainly compose of the s-AOs of Li and p-

AOs of Si. While its LUMO is the d-type orbitals, its HOMO is an s-type again composed of s-AOs of Li and Si. Consequently, Li_6Si (O_h) is expected to have an enhanced stability due to a closed electron shell configuration that satisfies the PSM. This analysis also points out that the Si dopant distributes all of its four valence electrons into the electron shell of Li_6Si . Similar observations are also found for the plots of DOS of Li_4Si and Li_5Si^+ (Figs. 1S and 2S in Supporting Information). Their eight valence electrons are occupied into the MOs following an electron shell ordering of $[1S^2 1P^6 1S^0]$. According to PSM, both Li_4Si and Li_5Si^+ are consistently the enhanced stability systems due to the eight valence electron configurations.

A legitimate question arises here as why both systems, Li_6Si containing 10 valence electrons and Li_4Si containing eight valence electrons, are the neutrals having an enhanced stability, whereas in the cationic state only Li_5Si^+ with eight valence electrons is the more stable. Although a local maximum peak appears at Li_7Si^+ in the plot of second-order difference in energy, its binding energy is quite low as compared to that of Li_5Si^+ .

Let us go back to the previous studies on the impure lithium clusters Li_nX . The shapes of the global minima of the more stable species Li_nX with $X = \text{B}, \text{Al}, \text{C}, \text{Ge}$, and Sn obtained from earlier reports are depicted in Figure 6. Stable systems for Li_nX with $X = \text{B}^{[8,9]}$ and $\text{Al}^{[10]}$ are found to be the eight valence electron species Li_5X (C_{4v}) in which the impurities B and Al are directly bound to five Li atoms. At the cationic state, Li_6X^+ (O_h , $X = \text{B}, \text{Al}$) in which X is bound to six Li atoms turns out to be the most stable species. Although being more stable as compared to the other sizes in the series of small clusters Li_nX ($n = 1-8$), the systems containing 10 valence electrons Li_7X and Li_8X^+ ($X = \text{B}, \text{Al}$) are less stable

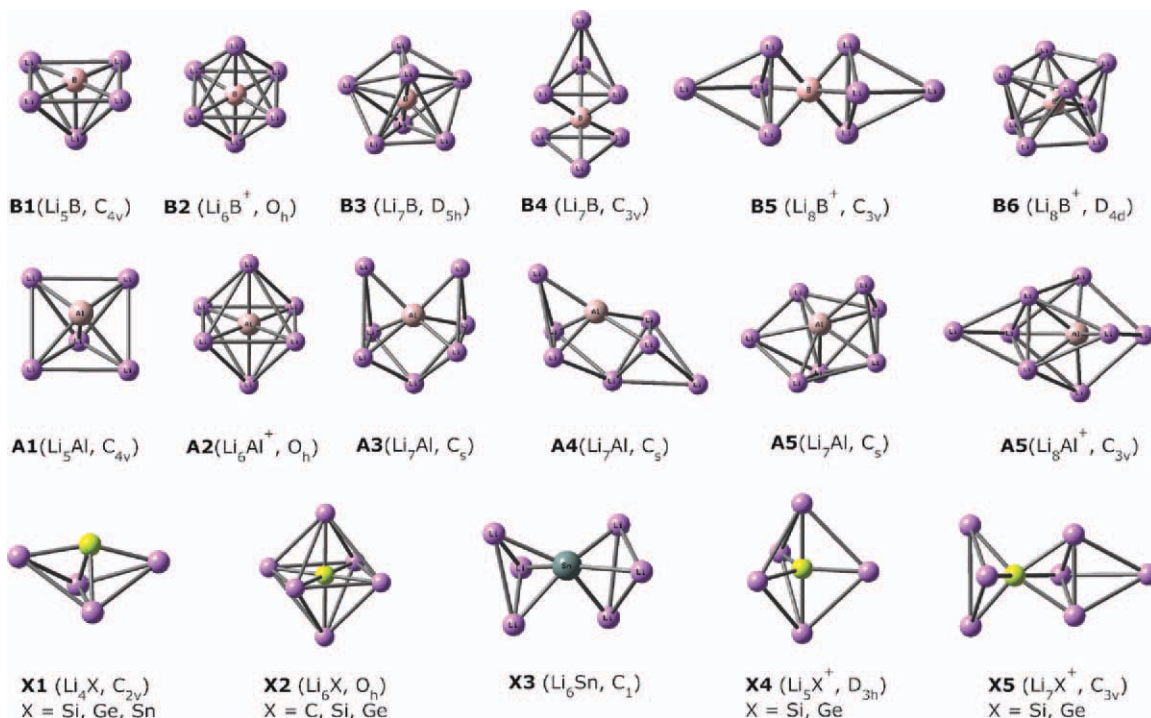


Figure 6. Shapes and symmetry of selected low-lying isomers for impure lithium clusters Li_nX with $X = \text{B}, \text{Al}, \text{C}, \text{Si}, \text{Ge}$, and Sn .

than the eight valence electron systems. Our previous studies on the Li_nB clusters revealed that the structures **B3** and **B4** are almost degenerate, whereas the structure **B5** is somewhat more stable than **B6** (Fig. 6). Similar observation was also found for Li_nAl in which the energetic difference between the structures **A3**, **A4**, and **A5** is very small. These less stable isomers either possess low symmetrical geometries or have a coordination number of the impurity lower than the number of Li atoms present. As a consequence, the enhanced stability is found for the species that possess the following characters: (i) a closed shell electronic configuration that satisfies the PSM, (ii) a high symmetry geometry, and (iii) the coordination number of impurity X is at least equal to the number of Li atoms.

To probe further these effects, the stabilities of group IVA-doped lithium clusters Li_nX with $\text{X} = \text{C}, \text{Si}, \text{Ge},$ and Sn are considered. In the neutral state, Li_6C (O_h) in which carbon with the coordination number of 6 was located at the center of the Li_6 cage, was experimentally and theoretically found to be the enhanced stability species.^[11,14–16] The same structure Li_6Si (O_h) is also demonstrated to have a special stability within the series of small clusters Li_nSi as discussed above. For small Li_nGe clusters, Ngan et al.^[13] showed that two systems Li_4Ge and Li_6Ge have high stability as compared to the other sizes. However, based on experimental results of mass spectroscopy of the cation Li_nGe^+ in which a high abundance was observed at the eight valence electron system Li_5Ge^+ , Li_4Ge is proposed to be more favored than Li_6Ge . From the theoretical results reported,^[13] it can be seen that the BE (E_b) of Li_6Ge (O_h) is slightly higher than that of Li_4Ge , whereas the second-order difference in total energy (Δ^2E) of these two systems is approximately equal. Thus, similar to results observed for Li_nSi clusters, both species Li_4Ge and Li_6Ge are the enhanced stability species within the series of small Li_nGe clusters. For the small clusters Li_nSn , Joshi and Kanhere^[12] reported that Li_4Sn exhibits a special stability within the series of small Li_nSn clusters, with high average binding energy, dissociation energy, and large HLG. In this case, Li_6Sn contains 10 valence electrons but has a low symmetrical geometry, and is thermodynamically less stable.

For cationic clusters, our theoretical predictions show that the Li_5Si^+ (D_{3h}) in which Si is directly bound to five Li atoms is actually the enhanced stability species. A similar system Li_5Ge^+ was also previously found by Ngan et al.^[13] In both cases, the 10 valence electron species Li_7X^+ ($\text{X} = \text{Si}, \text{Ge}$) have a C_{3v} structure in which one Li atom is capped on one triangular face of the octahedron Li_6X^+ . Consequently, the coordination number of the impurity X is lower than the number of Li atoms, and the Li_7X^+ is consistently less stable. These theoretical and experimental results lend a support for our proposal that the stability of a cluster not only does depend on the electron shell configurations but also is affected by the geometrical symmetry and the coordination number of the dopant.

Concluding Remarks

We have performed a systematic theoretical investigation on small silicon-doped lithium clusters Li_nSi ($n = 1\text{--}8$) at both

neutral and cationic states using high accuracy CCSD(T)/CBS approach. Location of the global minima was carried out using the stochastic search method, and growth mechanism of clusters was emphasized as follows:


- i. The small clusters Li_nSi with $n \leq 6$ are formed by directly binding one excess Li atom to Si atom of smaller cluster Li_{n-1}Si .
- ii. The structures tend to have an as high as possible symmetry and to maximize number of coordination of silicon. The first three-dimensional global minimum already appears at Li_4Si .
- iii. For larger clusters Li_7Si and Li_8Si , the global minima are formed by capping Li atoms on triangular faces of Li_6Si (O_h). The maximal number of coordination of silicon is found to be 6 for the global minima, and the structures with a higher number of coordination of silicon are less favorable.

Thermochemical properties such as heats of formation at 0 K ($\Delta_f H^0$) and 298 K ($\Delta_f H^{298}$), average binding energy (E_b), adiabatic (AIE) and vertical (VIE) ionization energies, dissociation energies (D_e), and second-order difference in total energy (Δ^2E) of the clusters in both neutral and cationic states are calculated from the CBS/CCSD(T) energies and used to evaluate relative stabilities of clusters. Our calculated results show that the species Li_4Si , Li_6Si , and Li_5Si^+ are characterized by an enhanced stability with large HLG, high binding energy, and second-order difference in total energy.

The enhanced stability of the species can be rationalized using the PSM but under the effects of some other factors including the geometrical symmetry and coordination number of the dopant. This proposal is extended to the clusters bearing other impurities Li_nX ($\text{X} = \text{B}, \text{Al}, \text{C}, \text{Si}, \text{Ge},$ and Sn). A consistent picture thus emerges on the structure and stability of doped Li clusters.

Keywords: lithium clusters • silicon-doped Li clusters • densities of states • electron shell model • cluster stability • heats of formation • ionization energy

How to cite this article: Tai TB, Nguyen MT, *J. Comput. Chem.* **2012**, 33, 800–809. DOI: 10.1002/jcc.22911

 Additional Supporting Information may be found in the online version of this article.

- [1] (a) W. D. Knight, K. Clemenger, W. A. de Heer, W. A. Saunders, M. Y. Chou, M. L. Cohen, *Phys. Rev. Lett.* **1984**, 52, 2141; (b) W. A. de Heer, *Rev. Mod. Phys.* **1993**, 65, 611.
- [2] K. Hoshino, K. Watanabe, Y. Konishi, T. Taguwa, A. Nakajima, K. Kaya, *Chem. Phys. Lett.* **1994**, 231, 499.
- [3] (a) W. Bouwen, F. Vanhoutte, F. Despa, S. Bouckaert, S. Neukermans, L. T. Kuhn, H. Weidele, P. Lievens, R. E. Silverans, *Chem. Phys. Lett.* **1999**, 314, 227; (b) E. Janssens, S. Neukermans, P. Lievens, *Curr. Opin. Solid State Mater. Sci.* **2004**, 15, 8.
- [4] (a) T. Höltzl, T. N. Veldeman, J. De Haeck, T. Veszpremi, P. Lievens, M. T. Nguyen, *Chem. Eur. J.* **2009**, 15, 3970; (b) T. Höltzl, T. Veszpremi, P. Lievens, M. T. Nguyen, *J. Phys. Chem. C* **2009**, 113, 21016; (c) V. T. Ngan, P. Gruene, P. Claes, E. Janssens, A. Fielicke, M. T. Nguyen, P. Lievens, *J. Am. Chem. Soc.* **2010**, 132, 15589.

- [5] (a) T. B. Tai, M. T. Nguyen, *Chem. Phys. Lett.* **2010**, 492, 292; (b) T. B. Tai, M. T. Nguyen, *Chem. Phys. Lett.* **2010**, 489, 75.
- [6] C. Yeretizian, *J. Phys. Chem.* **1995**, 99, 123.
- [7] M. Deshpande, A. Dhavale, R. R. Zope, S. Chacko, D. G. Kanhere, *Phys. Rev. A* **2002**, 6, 063202.
- [8] (a) Y. Li, D. Wu, Z. R. Li, C. C. Sun, *J. Comput. Chem.* **2007**, 28, 1677; (b) Y. Li, Y. J. Liu, D. Wu, Z. R. Li, *Phys. Chem. Chem. Phys.* **2009**, 11, 5703.
- [9] T. B. Tai, P. V. Nhat, M. T. Nguyen, S. Li, D. A. Dixon, *J. Phys. Chem. A* **2011**, 115, 7673.
- [10] T. B. Tai, P. V. Nhat, M. T. Nguyen, *Phys. Chem. Chem. Phys.* **2010**, 12, 11477.
- [11] P. Lievens, P. Thoen, S. Bouckaert, W. Bouwen, F. Vanhoutte, H. Weidele, R. E. Silverans, A. Navarro-Vazquez, P. v. R. Schleyer, *Eur. Phys. J. D* **1999**, 9, 289.
- [12] K. Joshi, D. G. Kanhere, *Phys. Rev. A* **2002**, 65, 043203.
- [13] (a) V. T. Ngan, J. D. Haack, H. T. Le, G. Gopakumar, P. Lievens, M. T. Nguyen, *J. Phys. Chem. A* **2009**, 113, 9080; (b) V. T. Ngan, P. Gruene, P. Claes, E. Janssens, A. Fielicke, M. T. Nguyen, P. Lievens, *J. Am. Chem. Soc.* **2010**, 132, 15589.
- [14] P. Lievens, P. Thoen, S. Bouckaert, W. Bouwen, F. Vanhoutte, H. Weidele, R. E. Silverans, A. N. Vazquez, P. v. R. Schleyer, *J. Chem. Phys.* **1999**, 110, 10316.
- [15] P. v. R. Schleyer, E. U. Wurthein, K. Kaufmann, T. Clark, A. Pople, *J. Am. Chem. Soc.* **1983**, 105, 5930.
- [16] H. Kudo, *Nature* **1992**, 355, 432.
- [17] P. Lievens, P. Thoen, S. Bouckaert, W. Bouwen, F. Vanhoutte, H. Weidele, R. E. Silverans, *Chem. Phys. Lett.* **1999**, 302, 571.
- [18] J. Ivanic, C. J. Marden, *J. Am. Chem. Soc.* **1993**, 115, 7503.
- [19] E. D. Jemmis, J. Chandrasekhar, E. U. Wurthein, P. v. R. Schleyer, J. W. Chin, F. J. Landro, R. J. Lagow, B. Luke, J. A. Pople, *J. Am. Chem. Soc.* **1982**, 104, 4275.
- [20] (a) S. Shetty, S. Pal, D. G. Kanhere, *J. Chem. Phys.* **2003**, 118, 7288; (b) K. Joshi, D. G. Kanhere, *J. Chem. Phys.* **2003**, 119, 12301; (c) K. Joshi, D. G. Kanhere, *Phys. Rev. A* **2002**, 65, 043203.
- [21] (a) P. v. R. Schleyer, J. Kapp, *Chem. Phys. Lett.* **1996**, 255, 363; (b) A. E. Reed, P. v. R. Schleyer, R. Janoschek, *J. Am. Chem. Soc.* **1991**, 113, 1885; (c) P. v. R. Schleyer, A. E. Reed, *J. Am. Chem. Soc.* **1988**, 110, 4454.
- [22] C. J. Marsden, *Chem. Phys. Lett.* **1995**, 245, 475.
- [23] Z. Shi, J. Wang, R. J. Boyd, *J. Phys. Chem.* **1995**, 99, 4941.
- [24] N. He, H. B. Xie, Y. H. Ding, *J. Comput. Chem.* **2008**, 11, 1850.
- [25] M. J. Frisch, G. W. Trucks, H. B. Schlegel, G. E. Scuseria, M. A. Robb, J. R. Cheeseman, J. A. Montgomery, Jr., T. Vreven, K. N. Kudin, J. C. Burant, J. M. Millam, S. S. Iyengar, J. Tomasi, V. Barone, B. Mennucci, M. Cossi, G. Scalmani, N. Rega, G. A. Petersson, H. Nakatsuji, M. Hada, M. Ehara, K. Toyota, R. Fukuda, J. Hasegawa, M. Ishida, T. Nakajima, Y. Honda, O. Kitao, H. Nakai, M. Klene, X. Li, J. E. Knox, H. P. Hratchian, J. B. Cross, V. Bakken, C. Adamo, J. Jaramillo, R. Gomperts, R. E. Stratmann, O. Yazyev, A. J. Austin, R. Cammi, C. Pomelli, J. Ochterski, P. Y. Ayala, K. Morokuma, G. A. Voth, P. Salvador, J. J. Dannenberg, V. G. Zakrzewski, S. Dapprich, A. D. Daniels, M. C. Strain, O. Farkas, D. K. Malick, A. D. Rabuck, K. Raghavachari, J. B. Foresman, J. V. Ortiz, Q. Cui, A. G. Baboul, S. Clifford, J. Cioslowski, B. B. Stefanov, G. Liu, A. Liashenko, P. Piskorz, I. Komaromi, R. L. Martin, D. J. Fox, T. Keith, M. A. Al-Laham, C. Y. Peng, A. Nanayakkara, M. Challacombe, P. M. W. Gill, B. G. Johnson, W. Chen, M. W. Wong, C. Gonzalez and J. A. Pople, *Gaussian 03 (Revision C.02)*; Gaussian, Inc.: Wallingford, CT, **2004**.
- [26] H.-J. Werner, P. J. Knowles, R. Lindh, F. R. Manby, M. Schütz, P. Celani, T. Korona, A. Mitrushenkov, G. Rauhut, T. B. Adler, R. D. Amos, A. Bernhardsson, A. Berning, D. L. Cooper, M. J. O. Deegan, A. J. Dobbyn, F. Eckert, E. Goll, C. Hampel, G. Hetzer, T. Hrenar, G. Knizia, C. Köppl, Y. Liu, A. W. Lloyd, R. A. Mata, A. J. May, S. J. McNicholas, W. Meyer, M. E. Mura, A. Nicklass, P. Palmieri, K. Pflüger, R. Pitzer, M. Reiher, U. Schumann, H. Stoll, A. J. Stone, R. Tarroni, T. Thorsteinsson, M. Wang, and A. Wolf, *MOLPRO*, version **2008.1**, a package of ab initio programs.
- [27] T. B. Tai, M. T. Nguyen, *J. Chem. Theory Comput.* **2011**, 7, 1119.
- [28] R. G. Parr, W. Yang, *Density-Functional Theory of Atoms and Molecules*; Oxford University Press: Oxford, **1989**.
- [29] A. D. Becke, *J. Chem. Phys.* **1993**, 98, 5648.
- [30] J. P. Perdew, J. A. Chevary, S. H. Vosko, K. A. Jackson, M. R. Pederson, D. J. Singh, C. Fiolhais, *Phys. Rev. B* **1992**, 46, 6671.
- [31] (a) J. D. Dill, J. A. Pople, *J. Chem. Phys.* **1975**, 62, 2921; (b) M. M. Francl, W. J. Pietro, W. J. Hehre, J. S. Binkley, M. S. Gordon, D. J. DeFrees, J. A. Pople, *J. Chem. Phys.* **1982**, 77, 3654.
- [32] R. Krishnan, J. S. Binkley, R. Seeger, J. A. Pople, *J. Chem. Phys.* **1980**, 72, 650.
- [33] J. Cizek, *Adv. Chem. Phys.* **1969**, 14, 35.
- [34] P. J. Knowles, C. Hampel, H. J. J. Werner, *Chem. Phys.* **1993**, 99, 5219.
- [35] K. Raghavachari, G. W. Trucks, J. A. Pople, M. Head-Gordon, *Chem. Phys. Lett.* **1984**, 1, 57.
- [36] T. H. Dunning, Jr., *J. Chem. Phys.* **1989**, 90, 1007.
- [37] D. E. Woon, T. H. Dunning, Jr., *J. Chem. Phys.* **1993**, 98, 1358.
- [38] K. A. Peterson, D. E. Woon, T. H. Dunning, Jr., *J. Chem. Phys.* **1994**, 100, 7410.
- [39] K. A. Peterson, T. H. Dunning, Jr., *J. Chem. Phys.* **2002**, 117, 10548.
- [40] (a) M. Douglas, N. M. Kroll, *Ann. Phys.* **1974**, 82, 89; (b) B. A. Hess, *Phys. Rev. A* **1985**, 32, 756; (c) B. A. Hess, *Phys. Rev. A* **1986**, 33, 3742.
- [41] W. A. de Jong, R. J. Harrison, D. A. Dixon, *J. Chem. Phys.* **2001**, 114, 48.
- [42] B. P. Prascher, D. E. Woon, K. A. Peterson, T. H. Dunning, A. K. Wilson, *Theor. Chem. Acc.* **2011**, 128, 60.
- [43] C. E. Moore, *Atomic energy levels as derived from the analysis of optical spectra*, Vol. 1, H to V; U.S. National Bureau of Standards Circular 467, U.S. Department of Commerce, National Technical Information Service, COM-72-50282: Washington, D.C., **1949**.
- [44] A. Karton, J. M. L. Martin, *J. Phys. Chem. A* **2007**, 111, 5936.
- [45] M. W. Chase, *J. Phys. Chem. Ref. Data. Monograph 9* **1998**, 2, 1.
- [46] L. A. Curtiss, K. Raghavachari, P. C. Redfern, J. A. Pople, *J. Chem. Phys.* **1997**, 106, 1063.
- [47] K. P. Huber, G. Herzberg, *Molecular Spectra and Molecular Structure Constants of Diatomic Molecules*; Van Nostrand-Reinhold: New York, **1979**.
- [48] A. I. Boldyrev, J. Simons, P. v. R. Schleyer, *J. Chem. Phys.* **1993**, 99, 8793.
- [49] M. W. Chase, Jr., *NIST-JANAF Thermochemical Tables*, 4th ed.; *J. Phys. Chem. Ref. Data, Monograph 9, Supplement 1*; American Institute of Physics: Woodbury, NY, **1998**.
- [50] R. W. Schmude, Q. Q. Ran, K. A. Gingerich, J. E. Kingcade, Jr., *J. Chem. Phys.* **1995**, 102, 2574.

Received: 10 October 2011
Revised: 18 November 2011
Accepted: 23 November 2011
Published online on 13 January 2012